


RESEARCH

Open Access



Research on fault tracing method of traction drive control system

Jintian Yin^{1,2*} , Zhilong He¹, Li Liu^{1,2}, Wu Shao^{1,2}, Hui Li^{1,2} and Dabing Sun^{1,2}

*Correspondence:
yinjintian0115@163.com

¹ School of Electrical Engineering,
Shaoyang University,
Shaoyang 422000, China

² Hunan Provincial Key
Laboratory of Grids Operation
and Control On Multi-Power
Sources Area, Shaoyang
University, Shaoyang 422000,
China

Abstract

Fault propagation is a common occurrence in traction drive control systems. The propagation of faults among components creates difficulties in traceability. Therefore, this paper focuses on the traction transmission control system and proposes a fault tracing method based on fault propagation. First, establish a fault propagation model that includes spatiotemporal characteristics. Then, extract the fault characteristics and the time it takes for faults to propagate at various observation points throughout system operation. Finally, match the spatiotemporal characteristics of the corresponding observation points in the fault propagation model, so as to determine the fault type and location, allowing for fault traceability. The proposed method's feasibility is verified using a system example. The effectiveness of the proposed method in the traction drive control system was verified through system examples, which can meet the requirements of rapid fault tracing and is effective for weak faults.

Keywords: Spatiotemporal characteristics, Fault propagation model, Fault tracing, Traction drive control system

Introduction

Fault diagnosis is a crucial method for monitoring the reliable and safe operation of complex systems. Fault tracing serves as a vital component of fault diagnosis to identify the type of fault and locate the fault location [1, 2]. Fault tracing technology has been extensively researched in various fields, including industrial process control and transportation equipment management. Due to the complex internal wiring of the traction control system, the interweaving of multiple physical fields, and the high coupling of functional and electrical connections between components, a fault occurring in one device will propagate to other locations, causing difficulties in identifying the origin of the fault [3, 4]. However, the current fault tracing of the traction control system of high-speed trains mainly focuses on diagnosing a single location of the traction control system when the device or subsystem malfunctions and lacks the study of the mechanism by which faults propagate. The study of the fault propagation features in the traction drive control system can, on the one hand, trace the root cause of faults and, on the other hand, find out the influence of different faults on the observed values of the position parameters of adjacent subsystems for monitoring [5].

Fault propagation is a common phenomenon in real systems, such as traffic jams, mass power faults in electrical systems, Internet outages, chemical, and chemical system accidents. Thesis [6] investigates on fault propagation by mining different effect trajectories in control loops for transient faults that are difficult to detect accurately in networked control systems. In Thesis [7], in the case of fault propagation among components in air handling systems, such as heating and air-conditioning, a dynamic hidden Markov model is used to identify fault modes, which effectively improves fault diagnosis accuracy. In Thesis [8], damage propagation modeling of aerogenerators is implemented. Thesis [9] proposed an improved symbolic transfer entropy and determination of weight threshold method to explore the fault propagation law and then traced the root cause of the fault by analyzing the information transfer changes between nodes and the fault propagation path. Paper [10] proposed a method that can efficiently generate a complete test set of double faults by analyzing the propagation paths of single faults and selecting undetected double faults to generate new test patterns, thus covering most of the double faults for a given current. Paper [11] described how mechanical disturbances on the drive shaft propagate from the disturbance torque to the current at the drive system supply input for mechanical faults in permanent magnet synchronous motor drive systems. Paper [12] proposed a new framework for a fault propagation path modeling method for power systems based on membrane computing and used an event-reinforced neural system to model the fault propagation path, which has the capability of graphical modeling and parallel knowledge reasoning to intuitively reveal the fault propagation path. By reviewing the literature, the current research on fault propagation is mainly focused on network systems, chemical industry, power systems, electronic circuits, etc., while the research oriented to traction drive control systems and traction motor fault propagation is rare.

Due to the intricate wiring of the traction drive control system, the interweaving of multiple physical fields, and the high coupling and high density of functional and electrical connections between components, it makes the fault propagation characteristics between system component units [13]. There are few studies on fault propagation and traceability for traction drive control systems and traction motors, and almost all studies on fault propagation are only from a spatial perspective without considering the temporal characteristics of fault propagation, while the occurrence, spread, propagation, and accumulation of system faults are time delayed [14]. The introduction of time into the study of fault propagation can provide a more realistic and accurate description of the system fault propagation, and the proposed methods such as fault diagnosis or sensor arrangement related to the time factor will be more reasonable on this basis [15, 16]. Therefore, analyzing the temporal features of fault propagation is imperative.

In addition, fault propagation in traction drive control systems is characterized by its dynamic nature and diversity of fault modes, which presents significant challenges in developing fault propagation models and conducting analyses. The dynamic nature refers to the operating condition of the traction drive control system, that is, the variable speed of the train when a fault occurs and propagates; the diversity of fault modes means that many types of faults can occur in the traction drive control system, which can be divided into traction motor faults, variable flow faults such as device faults, TCU (traction drive control unit) faults, and sensor faults, and each major fault can be divided into

several fault types. Different fault types may correspond to different fault causes, and the same fault cause may cause multiple fault types. This increases the difficulty of fault analysis in the traction control system. In addition, conducting fault tracing research on weak faults can effectively avoid the occurrence of major accidents, help organize and arrange maintenance on site, and have significant economic and social benefits. This paper mainly studies the propagation of traction motor faults in the traction drive control system.

Traction drive control system fault propagation modeling

Generic model

Set up Q observation points at various locations of the traction drive control system (the observation points should be placed based on the structural characteristics of the system, utilize the available sensor conditions, and establish them at measurable positions) and establish the signal propagation model of p observation points during normal operation of the system.

$$Z_p(t_p) = S_{p,p-1} \cdot Z_{p-1}(Z_{p-1}) \tag{1}$$

where $S_{p,p-1} = f(G_{p,p-1}, t_p)$ Q denotes the signal at the $Z_p(t_p)$ $p(p = 1, 2, \dots, Q)$ observation point, which can be various physical quantities such as current and voltage; $Z_{p-1}(t_{p-1})$ denotes the signal at the $p - 1$ observation point; t_p and t_{p-1} denote the time variables at the p and $p - 1$ observation points, respectively; $t_p = t_{p-1} + \Delta t_{p,p-1}$ and $\Delta t_{p,p-1}$ are the time required for the signal at the $p - 1$ observation point to propagate to the p observation point; and $S_{p,p-1}$ denotes the transfer function from the signal at the $p - 1$ observation point $Z_{p-1}(t_{p-1})$ to the signal at the p observation point $Z_p(t_p)$, where $G_{p,p-1}$ is determined by the system structure between the two observation points; when $p = 1$, $Z_1(t_1) = S_{1,0} \cdot Z_0(t_0)$ is set at the $p = 0$ point at the Q th observation point, i.e., $Z_0(t_0) = Z_Q(t_Q)$ means that the signal propagation forms a closed loop, and $S_{1,0}$ indicates the transfer function from $p = Q$ signal $Z_Q(t_Q)$ propagation to the point $Z_1(t_1)$ with $p = 1$; if the point $p = 0$ is set at the power supply or traction motor, it means that the signal propagation from the observation point $p = 0$ to the observation point Q occurs in an open-loop format. Equation (1) uses the signal at the $p - 1$ observation point to characterize the signal at the p observation point, that is, the signal at the p observation point is propagated from the signal at the $p - 1$ observation point. Similarly, $Z_{p-1}(t_{p-1}) = S_{p-1,p} \cdot Z_p(t_p)$ and $S_{p-1,p}$ represent the transfer function from the signal at the observation point p $Z_p(t_p)$ to the signal at observation point $p - 1$ $Z_{p-1}(t_{p-1})$.

Equation (1) can be described as follows:

$$Z_p(t_p) = S_{p-1,p} \cdots S_{2,1} \cdot S_{1,0} \cdot Z_0(t_0) = S_{i,i-1} \cdot Z_0(t_0) \tag{2}$$

Equation (2) characterizes the signal at the p observation point by the signal at $= 0$ $Z_0(t_0)$, i.e., the signal at the p observation point is propagated from $Z_0(t_0)$ through $Z_1(t_1)$, $Z_2(t_2)$, and $Z_{p-1}(t_{p-1})$.

When a fault occurs in the traction drive control system, the p observation point signal is expressed as follows: $\sum_{fp,h}^k (t_{fp}^k) = z_p(t_{fp}^k) \oplus z_{fp,h}^k [f_h^k(\cdot), S_{p,h}, t_{fp}^k]$ (3).

where $Z_p(t_{fp}^k)$ is the signal at the observation point of p during normal operation of the traction drive control system; $Z_p(t_{fp}^k) = Z_p(t_p) Z_{fp,h}^k(t_{fp}^k)$ is the signal at the observation point of when a fault of type k occurs at p k h , where $k = 1, 2, \dots, n_f$ indicates the type of fault in the traction drive control system (different locations of the same component are considered as different types of faults) and h is the location of the fault (different types of faults may have the same location in the system), $h = 1, 2, \dots, n_g$; $S_{p,h}$ is the signal transfer function from the fault location h to the observation point; $f_h^k(\cdot)$ is the $z_{fp,h}^k$ which is the source signal of the fault in the traction drive control system at the point h when a fault of type k occurs; t_{fp}^k is the time variable at the observation point; $z_{fp,h}^k [f_h^k(\cdot), S_{p,h}, t_{fp}^k]$ is the evolving fault signal propagated by the source signal $f_h^k(\cdot)$ from the point h to the observation point p and is a function of $f_h^k(\cdot), S_{p,h}$ and t_{fp}^k ; and $z_{fp,h}^k$ is the signal operation, which can be summing or multiplying, i.e., the signal at the observation point p after a fault occurs in the system is obtained by summing or multiplying the signal without the fault signal part $Z_p(t_{fp}^k)$ with the evolving fault signal $z_{fp,h}^k$

$$z_{fp,h}^k(t_{fp}^k) = Z_p(t_{fp}^k) + (t_{fp}^k) + z_{fp,h}^k [f_h^k(\cdot), S_{p,h}, t_{fp}^k] \tag{4}$$

or

$$z_{fp,h}^k(t_{fp}^k) = Z_p(t_{fp}^k) * z_{fp,h}^k [f_h^k(\cdot), S_{p,h}, t_{fp}^k] \tag{5}$$

The p observation point time variable t_{fp}^k can be expressed as $t_{fp}^k = t_h^k + \Delta t_{fp}^k$, t_h^k is the time variable at the system fault point h , and Δt_{fp}^k is the time required for the propagation of the type k fault signal from the fault point h to the observation point p . According to the composition of the execution time of the system for the signal, the propagation time of the fault signal Δt_{fp}^k includes the signal input processing time T_1 , the control strategy operation time T_2 , and the control operation output processing time T_3 .

For the fault source signal $f_h^k(\cdot)$ in Eq. (3), according to the traction drive control system fault scenario, the following equation can be expressed as follows:

$$f_h^k(\cdot) = \sum^N \sum^{n_j} [\Gamma(t - (T_{tj} + T_{cj} * \tau_j) - T_{cj} * (l - 1)) - \Gamma(t - T_{tj} - T_{cj} * (l - 1))] * TH\{cs_k\} \tag{6}$$

where Γ is the step function, N is the number of different types of pulse sequences, j is the number of pulse sequences of j , n_j is the total number of pulse signals of j , $n_j = \text{ceil} \left(\frac{(T_{t(j+1)} - T_{tj})}{T_{cj}} \right)$ and ceil are rounded to positive infinity, T_{cj} is the subperiod (the fault signal of j), τ_j is the operating period (the pulse sequence), $j TH\{\}$ is the threshold function, T_{tj} is the trigger moment (the fault signal of j), cs_j is the fault state (the fault signal of j), $cs_j = 0$ is the open-circuit fault, and $cs_j = 1$ is the short circuit fault. The equation can represent various fault conditions, such as transient, intermittent, permanent, and their combinations, where $\tau_j \rightarrow 0$ means the fault is transient, $0 < \tau_j < 1$ means the fault is intermittent, and $\tau_j \rightarrow 1$ means the fault is permanent.

Common faults in the traction drive control system

(1) Traction motor fault

When the traction motor faults, $f(\cdot)$ can be given by the following Eq. [17]:

$$F(\cdot) = cs_j(M, f_1, s) = A_1(M) * \cos(2\pi f_{s1}t + \theta_1) + A_2(M) * \cos(2\pi f_{s2}t + \theta_2), 0 \leq M \leq 1 \tag{7}$$

where M indicates the severity of the fault; $M = 0$ indicates no fault in the traction motor; $M = 1$ indicates a completely broken rotor guide bar in the traction motor; A_1 and A_2 are the magnitudes of the side frequency current components, whose magnitudes are proportional to M ; f_1 is the fundamental frequency of the current; s is the rate of rotation; f_{s1} and f_{s2} are the fault characteristic frequencies (contained in the stator current in case of a broken bar fault); and $f_{s1} \approx f_{s2}$ and $f_{s1} = g_1(f_1, s)$ and θ_1 and θ_2 are the initial phase angles of the side frequency components.

According to the traction motor fault mechanism analysis as follows:

1) Broken rotor bar fault, $f_s = (1 \pm 2ks)f_1$, is its fault characteristic frequency; in that case, the fault signal $f(\cdot)$ is expressed as follows.

$$f(\cdot) = cs_j(M, f_1, s) = A_1(M) * \cos[2\pi(1 - 2ks)f_1t + \theta_1] + A_2(M)\cos[2\pi(1 - 2ks)f_1t + \theta_2] \tag{8}$$

2) Stator turn-to-turn short circuit fault, $f_s = [n \pm 2k(1 - 2s)]f_1$, is its fault characteristic frequency; in that case, the fault signal $f(\cdot)$ is expressed as follows:

$$f(\cdot) = cs_j(M, f_1, s) = A_1(M) * \cos\{2\pi[n + 2k(1 - 2s)]f_1t + \theta_1\} + A_2(M)\cos\{2\pi[n - 2k(1 - 2s)]f_1t + \theta_2\} \tag{9}$$

(3) Air gap eccentricity fault, $f_s = [n \pm k(1 - s)]f_1$, is its fault characteristic frequency; in that case, the fault signal $f(\cdot)$ is expressed as follows:

$$f(\cdot) = cs_j(M, f_1, s) = A_1(M) * \cos\{2\pi[n + k(1 - s)]f_1t + \theta_1\} + A_2(M)\cos\{2\pi[n - k(1 - s)]f_1t + \theta_2\} \tag{10}$$

(4) End-loop fracture fault, $f_s = (1 \pm 2ks)f_1$, is its fault characteristic frequency; in that case, the fault signal $f(\cdot)$ is expressed as follows:

$$f(\cdot) = cs_j(M, f_1, s) = A_1(M)*\cos[2\pi(1 - 2ks)f_1t + \theta_1]+A_2(M)\cos[2\pi(1 + 2ks)f_1t + \theta_2] \tag{11}$$

(2) Converter fault

The main converter faults are power device failure faults, power device and passive component electrical characteristic degradation faults, passive component failure faults, etc. The power device fault is as described in (6); for the power device and passive component electrical characteristic degradation fault, $f(\cdot) = f(\xi)$ and ξ denote the electrical characteristic degradation rate; for the passive component, fault $f(\cdot) = conts$ and $conts$ are arbitrary constants.

(3) Sensor fault

The CRH2 high-speed train traction drive control system fault types mainly include deviation, drift, shock, accuracy degradation, periodic disturbance, gain, open circuit,

short circuit, stuck and nonlinear dead zone faults of voltage, current, and speed sensors. When a sensor failure occurs, $cs_j(\cdot)$ can be given by the following equation, $cs_j(c) = c$, where c is a constant real number.

1) In the case of sensor deviation fault, the expression of the fault signal $f(\cdot)$ is shown in the following equation.

$$f(Conts) = Conts \tag{12}$$

2) In the case of sensor drift fault, the expression of the fault signal $f(\cdot)$ is shown in the following equation.

$$f(a) = a * t \tag{13}$$

3) In the case of sensor shock fault, the expression of the fault signal $f(\cdot)$ is shown in the following equation.

$$f(t) = \delta(t) \tag{14}$$

where $\delta(t)$ is the shock signal.

(4) Traction controller fault

Common fault types of traction controllers include faulty logic states or hard damage in analog signal I/O modules, digital signal I/O modules, and memory modules.

1) For analog signal I/O module fault, the expression of the fault signal $f(\cdot)$ is shown in the following equation.

$$f(p, q, A) = A(e^{pt} - e^{qt}) \tag{15}$$

where p and q denote the time coefficients by which the rising and falling edge times and the width of the pulse are determined and A denotes the magnitude of the amplitude.

2) For digital signal I/O module fault, compare the pin level threshold TH with the instantaneous pulse signal; if the latter is large, then $f(\cdot) = 1$; otherwise, $f(\cdot) = 0$.

3) For memory module fault, $f(\cdot)$ is the random bit flip value of the speed sensor feedback signal (moment of fault).

Actual fault case analysis CRH2 high-speed train traction drive control system consists of traction transformer, pulse rectifier, intermediate DC link, traction inverter, traction motor, and controller, and the traction motor is a three-phase squirrel cage asynchronous motor. Four observation points are sequentially established on the system. The system's structure and observation points are outlined in Fig. 1, while the main circuit topology of the traction drive control system is featured in Fig. 2.

The current signal analysis method is widely used for analyzing faults in the traction drive control system. Through the examination of the circuit structure and modulation theory, it can derive the current signal model for observation point 2 and observation point 4 in the system.

$$\begin{cases} Z_2(t_2)S_{2,1} \cdot Z_1(t_1) \\ Z_4(t_4)S_{4,e} \cdot Z_3(t_3) \end{cases} \tag{16}$$

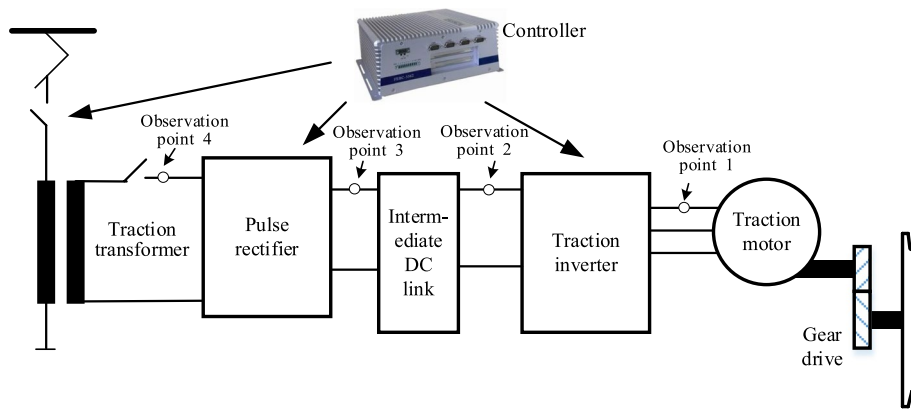


Fig. 1 Diagram of observation points of the traction drive control system

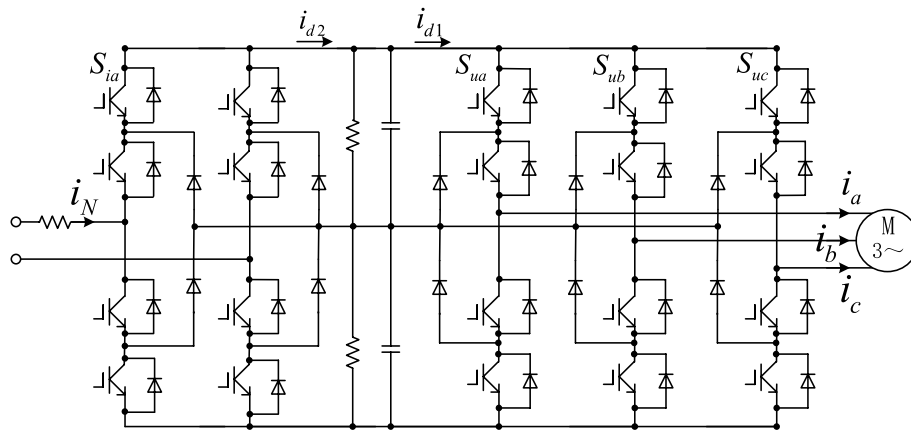


Fig. 2 Main circuit topology of traction drive control system

where $Z_1(t_1) = [i_a i_b i_c]^{-1}$ and $S_{2,1} = [S_{ua} S_{ub} S_{uc}] S_{ua} S_{ub}$, and S_{uc} are inverter three-phase switching functions; $S_{4,3} = S_{ia}$ are rectifier switching functions, and i_a , i_b , and i_c are inverter output currents (i.e., traction motor stator currents); $Z_2(t_2) = i_{d1}$ are inverter input currents; $Z_3(t_3) = i_{d2}$ are rectifier output currents; and $Z_4(t_4) = i_N$ are rectifier input side currents.

The inverter three-phase switching function can be obtained by utilizing the double Fourier transform as follows [18].

$$\begin{aligned}
 S_{ua} = & \frac{M}{2} \cos(\omega_1 t_2) + \frac{2}{\pi} \sum_{m=1}^{\infty} \frac{1}{m} J_0\left(\frac{\pi}{2} m M\right) \sin\left(\frac{\pi}{2} m\right) \cos(m \omega_c t_2) \\
 & + \frac{2}{\pi} \sum_{m=1}^{\infty} \sum_{\substack{n=-\infty \\ n \neq 0}}^{\infty} \frac{1}{m} J_n\left(\frac{\pi}{2} m M\right) \sin\left[\frac{\pi}{2}(m+n)\right] \cos(m \omega_c t_2 + n \omega_1 t_2) \quad (17)
 \end{aligned}$$

$$\begin{aligned}
 S_{ub} = & \frac{1}{2} + \frac{M}{2} \cos\left(w_1 t_2 - \frac{2\pi}{3}\right) + \frac{2}{\pi} \sum_{m=1}^{\infty} \frac{1}{m} J_0\left(\frac{\pi}{2} m M\right) \sin\left(\frac{\pi}{2} m\right) \cos(\omega_c t_2) \\
 & + \frac{2}{\pi} \sum_{m=1}^{\infty} \sum_{\substack{n=-\infty \\ n \neq 0}}^{\infty} \frac{1}{m} J_n\left(\frac{\pi}{2} m M\right) \sin\left[\frac{\pi}{2}(m+n)\right] \cos\left[m\omega_c t_2 + n\left(\omega_1 t_2 - \frac{2\pi}{3}\right)\right] \quad (18)
 \end{aligned}$$

$$\begin{aligned}
 S_{uc} = & \frac{1}{2} + \frac{M}{2} \cos\left(w_1 t_2 - \frac{2\pi}{3}\right) + \frac{2}{\pi} \sum_{m=1}^{\infty} \frac{1}{m} J_0\left(\frac{\pi}{2} m M\right) \sin\left(\frac{\pi}{2} m\right) \cos(\omega_c t_2) \\
 & + \frac{2}{\pi} \sum_{m=1}^{\infty} \sum_{\substack{n=-\infty \\ n \neq 0}}^{\infty} \frac{1}{m} J_n\left(\frac{\pi}{2} m M\right) \sin\left[\frac{\pi}{2}(m+n)\right] \cos\left[m\omega_c t_2 + n\left(\omega_1 t_2 - \frac{2\pi}{3}\right)\right] \quad (19)
 \end{aligned}$$

where ω_1 is the modulating wave angular frequency, ω_c is the carrier angular frequency, M is the modulation system, m is the carrier frequency multiplier, n is the modulating wave harmonic frequency multiplier, J_0 and J_n are the first type of Bessel functions, and t_2 is the intermediate DC link observation point 2 time variable.

Rectifier *a* bridge arm switching function [19].

$$\begin{aligned}
 S_{ia} = & \sum_{n=1}^{\infty} \frac{4}{\pi} \left[\frac{1}{2n-1} \sin(2n-1)\theta \cos(2n-1)\omega t_4 + \frac{1}{2n-1} \cos(2n-1)\theta \sin(2n-1)\omega t_4 \right] \\
 = & \frac{4}{\pi} \sin(\omega t_4 - \theta) + \frac{4}{\pi} \sum_{n=1}^{\infty} \frac{1}{4n \pm 1} \sin[(4n \pm 1)\omega t_4 - (4n \pm 1)\theta] (n = 1, 2, 3, \dots) \quad (20)
 \end{aligned}$$

where θ is the rectifier control angle; ω is the angular frequency of the power supply, and the corresponding frequency is $f\omega$; and t_4 is the rectifier input side time variable.

The stator three-phase current of the traction motor at normal fault-free time is expressed as follows [20]:

$$\begin{cases} i_a = I_m \cos(\omega_1 t - \varphi) \\ i_b = I_m \cos\left(\omega_1 t - \varphi - \frac{2}{3}\pi\right) \\ i_c = I_m \cos\left(\omega_1 t - \varphi + \frac{2}{3}\pi\right) \end{cases} \quad (21)$$

where I_m and φ are the amplitude and phase of the fundamental component of the stator current, respectively, ω_1 is the angular frequency of the voltage applied to the motor, and ω_1 corresponds to the frequency of f_1 .

Broken rotor bar happens most frequently in rotor faults with an occurrence probability of 10% of the total fault of the traction motor. Assuming that the fault type is $k = 1$ and the fault location is $h = 1$, the fault source signal of Eq. (6) when the broken bar fault occurs in the traction motor is expressed as follows [17]:

$$f_1^1(\cdot) = I_{bp} \cos(2\pi f_{s1} t - \varphi_{bp}) + I_{bn} \cos(2\pi f_{s2} t - \varphi_{bn}) \quad (22)$$

where f_{s1} and f_{s2} are the fault characteristic frequencies and $f_{s1} = (1 + 2s)f_1$ and $f_{s2} = (1 - 2s)f_1$ [21, 22]; I_{bp} , I_{bn} , φ_{bp} , and φ_{bn} are the amplitude and phase of the $(1 + 2s)f_1$ frequency component and $(1 - 2s)f_1$ frequency component, respectively; and s is the slip rate.

At this point, the three-phase stator current of the traction motor (observation point 1) can be expressed as follows:

$$\begin{cases} Z_{f1a,1}^1(t_{f1}^1) = i_a = I_m \cos(\omega_1 t_{f1}^1 - \varphi) + I_{bp} \cos[(1 + 2s)\omega_1 t_{f1}^1 - \varphi_{bp}] + I_{bn} \cos[(1 - 2s)\omega_1 t_{f1}^1 - \varphi_{bn}] \\ Z_{f1b,1}^1(t_{f1}^1) = i_b = I_m \cos(\omega_1 t_{f1}^1 - \varphi - \frac{2}{3}\pi) + I_{bp} \cos[(1 + 2s)\omega_1 t_{f1}^1 - \varphi_{bp}] \\ \quad + I_{bn} \cos[(1 - 2s)\omega_1 t_{f1}^1 - \varphi_{bn} - \frac{2}{3}\pi] \\ Z_{f1c,1}^1(t_{f1}^1) = i_c = I_m \cos(\omega_1 t_{f1}^1 - \varphi + \frac{2}{3}\pi) + I_{bp} \cos[(1 + 2s)\omega_1 t_{f1}^1 - \varphi_{bp} + \frac{2}{3}\pi] \\ \quad + I_{bn} \cos[(1 - 2s)\omega_1 t_{f1}^1 - \varphi_{bn} + \frac{2}{3}\pi] \end{cases} \tag{23}$$

Combining with Eq. (3), the a-phase current at observation point 1 is as follows.

$$Z_1(t_{f1}^1) I_m \cos(\omega_1 t_{f1}^1 - \varphi)$$

$$Z_{f1,1}^1[f_1^1(\cdot), S_{1,1}, t_{f1}^1] = I_{bp} \cos[(1 + 2s)\omega_1 t_{f1}^1 - \varphi_{bp}] + I_{bn} \cos[(1 - 2s)\omega_1 t_{f1}^1 - \varphi_{bn}]$$

$Z_{f1,1}^1(t_{f1}^1) = Z_1(t_{f1}^1) + Z_{f1,1}^1[f_1^1(\cdot), S_{1,1}, t_{f1}^1]$, which is consistent with Eq. (4); the phase b and c currents are similar to the phase a current.

Substituting Eqs. (17), (18), (19), and (23) into Eq. (16) yields the expression for the current signal at observation point 2.

$$\begin{aligned} Z_{f2,1}^1(t_{f2}^1) &= i_{d1} = \frac{3}{4} MI_m \cos\varphi + \frac{3}{4} M [I_{bp} \cos(2s\omega_1 t_{f2}^1 + \varphi_{bp}) + I_{bn} \cos(2s\omega_1 t_{f2}^1 + \varphi_{bn})] \\ &\quad + \sum_{m=1}^{\infty} \sum_{n=-\infty}^{\infty} \frac{2}{m\pi} J_n\left(\frac{\pi}{2} M\right) \sin\left[(m+n)\frac{\pi}{2}\right] \left\{ \cos(m\omega_c t_{f2}^1 + n\omega_1 t_{f2}^1) i_a \right. \\ &\quad \left. + \cos\left[m\omega_c t_{f2}^1 + n\left(\omega_1 t_{f2}^1 - \frac{2}{3}\pi\right)\right] i_b + \cos\left[m\omega_c t_{f2}^1 + n\left(\omega_1 t_{f2}^1 + \frac{2}{3}\pi\right)\right] i_c \right\} \\ &= \frac{3}{4} MI_m \cos\varphi + \frac{3}{4} MI_{2s} \cos(2s\omega_1 t_{f2}^1 - h) + i_h \end{aligned} \tag{24}$$

where $\frac{3}{4} MI_m \cos\varphi$ is the DC component, $I_{2s} = \sqrt{I_{bp}^2 + I_{bn}^2 + 2I_{bp}I_{bn}\cos(\varphi_{bp} + \varphi_{bn})}$ is the component amplitude of the frequency $2sf_1$, $h = \arctan \frac{I_{bn}\sin\varphi_{bn} - I_{bp}\sin\varphi_{bp}}{I_{bn}\cos\varphi_{bn} - I_{bp}\sin\varphi_{bp}}$ is the component phase of the frequency $2sf_1$, and i_h is the high frequency component of the summation symbol.

Combining with Eq. (3), the current signal at observation point 2 is as follows.

$$Z_2(t_{f2}^1) = \frac{3}{4} MI_m \cos\varphi + i_h$$

$$Z_{f2,1}^1[f_1^1(\cdot), S_{2,1}, t_{f2}^1] = \frac{3}{4} MI_{2s} \cos(2s\omega_1 t_2 - h)$$

$$Z_{f2,1}^1(t_{f2}^1) = Z_2(t_{f2}^1) + Z_{f2,1}^1[f_1^1(\cdot), S_{2,1}, t_{f2}^1]$$

$Z_{f2,1}^1(t_{f2}^1) = Z_2(t_{f2}^1) + Z_{f2,1}^1[f_1^1(\cdot), S_{2,1}, t_{f2}^1]$, which is consistent with Eq. (4).

In the traction drive control system, observation point 2 and observation point 3 have essentially the same time variable, i.e., $t_{f2}^1 \approx t_{f3}^1$. Since the intermediate DC link

Table 1 Frequency values of fault characteristics at different observation points

Grid frequency f (Hz)	Motor stator current frequency f_1 (Hz)	Slip rate s	Observation point 1 current fault characteristic frequency $(1 \pm 2s)f_1$ (Hz)	Observation point 2 current fault characteristic frequency $2sf_1$ (Hz)	Observation point 2 current fault characteristic frequency $2sf_1$ (Hz)	Observation point 4 current fault characteristic frequency $(4n \pm 1)f \pm 2sf_1$ (Hz)
50	131.1	0.0172	126.6/135.6	4.5	4.5	45.5/54.5 145.5/154.5 245.5/254.5

capacitor actually plays the role of low-pass filtering, the high-frequency component of i_{d1} in Eq. (4) will be filtered out, containing only the low-frequency component and the DC component; therefore, the observation point 3 current signal can be known by the observation point 2 signal expressed as follows:

$$Z_{f3,1}^1(t_{f3}^1) = i_{d2} = \frac{3}{4}MI_m \cos\varphi + \frac{3}{4}MI_{2s} \cos(2s\omega_1 t_{f3}^1 - h) \tag{25}$$

Therefore, at observation point 2 and observation point 3, $2sf_1$ is the characteristic frequency of a weak fault in the pre-breakage period of the traction motor.

Combining with Eq. (3), the current signal at observation point 3 is as follows:

$$Z_3(t_{f3}^1) = \frac{3}{4}MI_m \cos\varphi$$

Table 2 Time required for propagation of different faults in the traction drive control system to different observation points

		Fault feature propagation to different observation points experience time $\Delta_{p,h}^k$			
		Observation point 1	Observation point 2	Observation point 3	Observation point 4
Fault type	Traction motor failure	$0 T_1 + T_2 + T_3$	$T_1 + T_2 + T_3$	$T_1 + T_2 + T_3$	$2(T_1 + T_2 + T_3)$
	TCU external communication port has analog and digital interference	$T_2 + T_3$	$T_2 + T_3$	$T_2 + T_3$	$T_2 + T_3$
	TCU output control signal abnormal	T_3	T_3	T_3	T_3
	Speed sensor failure, stator current sensor failure	0	$T_1 + T_2 + T_3$	$T_1 + T_2 + T_3$	$T_1 + T_2 + T_3$
	Rectifier input side current sensor, intermediate DC link current sensor fault	$T_1 + T_2 + T_3$	$T_1 + T_2 + T_3$	$T_1 + T_2 + T_3$	$T_1 + T_2 + T_3$
	Rectifier input side voltage sensor, intermediate DC link voltage sensor failure	$T_1 + T_2 + T_3$	$T_1 + T_2 + T_3$	$T_1 + T_2 + T_3$	$T_1 + T_2 + T_3$
	Inverter power device failure or deterioration of electrical characteristics	T_3	T_3	T_3	$T_1 + T_2 + 2T_3$
	Failure of rectifier power devices or deterioration of electrical characteristics	$T_1 + T_2 + 2T_3$	T_3	T_3	T_3
	Passive component failure or deterioration of electrical characteristics	$T_1 + T_2 + T_3$	0	0	$T_1 + T_2 + T_3$

$$Z_{f3,1}^1 [f_1^1(\cdot), S_{3,1}, t_{f3}^1] = \frac{3}{r} MI_{2s} \cos(2s\omega_1 t_{f3}^1 - h)$$

$$Z_{f3,1}^1 (t_{f3}^1) = Z_3 (t_{f3}^1) + Z_{f3,1}^1 [f_1^1(\cdot), S_{3,1}, t_{f3}^1], \text{ which is consistent with Eq. (4).}$$

Equations (20) and (25) are substituted into Eq. (16) to obtain the expression for the current signal at observation point 4.

$$\begin{aligned} Z_{f4,1}^1 (t_{f4}^1) = & i_N \frac{3}{2\pi} M \left\{ I_m \sin(\omega_1 t_{f4}^1 - \theta \pm \varphi) + I_{2s} \sin[(\omega \pm 2s\omega_1) t_{f4}^1 - \theta \mp h] \right. \\ & + \frac{1}{4n \pm 1} \sum_{n=1}^{\infty} I_m \sin[(4n \pm 1)\omega t_{f4}^1 - (4n \pm 1)\theta \mp \varphi] \\ & \left. + \frac{1}{4n \pm 1} \sum_{n=1}^{\infty} I_{2s} \sin[(4n \pm 1)\omega t_{f4}^1 \pm 2s\omega_1 t_{f4}^1 - (4n \pm 1)\theta \mp h] \right\} \end{aligned} \tag{26}$$

Therefore, at observation point 4, $(4n \pm 1)f \pm 2sf_1$ is the characteristic frequency of the traction motor for the occurrence of a pre-fault with broken rotor bars.

Combining with Eq. (3), the current signal at observation point 4 is as follows:

$$Z_4 (t_{f4}^1) = \frac{3}{2\pi} M \left\{ I_m \sin(\omega t_{f4}^1 - \theta \mp \varphi) + \frac{1}{4n \pm 1} \sum_{n=1}^{\infty} I_m \sin[(4n \pm 1)\omega t_{f4}^1 - (4n \pm 1)\theta \mp \varphi] \right\}$$

$$\begin{aligned} Z_{f4,1}^1 [f_1^1(\cdot), S_{4,1}, t_{f4}^1] = & \frac{3}{2\pi} M \left\{ I_{2s} \sin[(\omega \pm 2s\omega_1) t_{f4}^1 - \theta \mp h] \right. \\ & \left. + \frac{1}{4n \pm 1} \sum_{n=1}^{\infty} I_{2s} \sin[(4n \pm 1)\omega t_{f4}^1 \pm 2s\omega_1 t_{f4}^1 - (4n \pm 1)\theta \mp h] \right\} \end{aligned}$$

$$S_{f4,1}^1 (t_{f4}^1) = Z_4 (t_{f4}^1) + Z_{f4,1}^1 [f_1^1(\cdot), S_{4,1}, t_{f4}^1], \text{ which is consistent with Eq. (4).}$$

The frequency of fault characteristics at different observation points of the traction drive control system reflects the spatial characteristics of fault propagation.

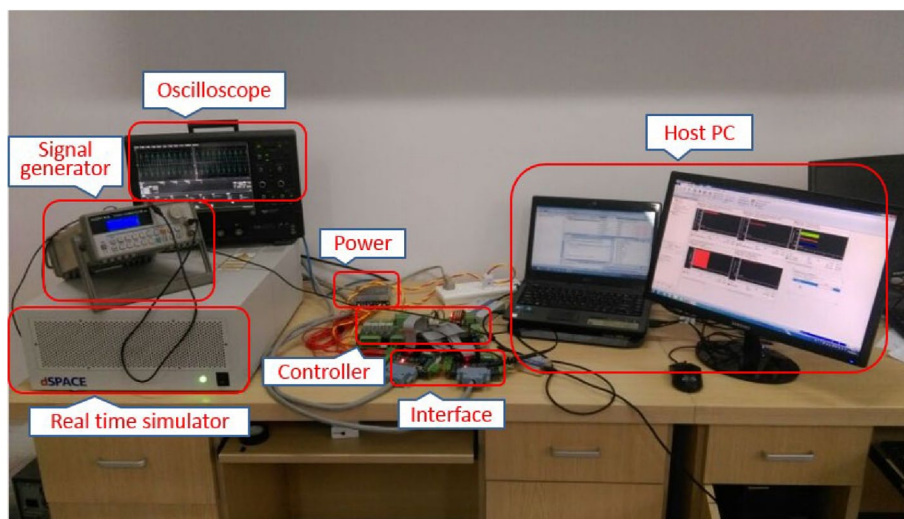


Fig. 3 CRH2 traction drive control system semi-physical platform

According to the system parameters and motor parameters of the CRH2 traction drive control system operating at 200 km/h speed, the fault characteristic frequency values of different observation points when the traction motor rotor of the traction drive control system is weakly faulty in the pre-breakage period are calculated by combining the above conclusions, as shown in Table 1.

According to the execution time of the system on the signal, Eqs. (23) to (26) are as follows:

$$\begin{aligned}
 t_{f2}^1 &= t_1^1 + \Delta t_{f2,1}^1, \Delta t_{f2,1}^1 = T_1 + T_2 + T_3, t_{f2}^1 = t_1^1 + (T_1 + T_2 + T_3). \\
 t_{f3}^1 &= t_1^1 + \Delta t_{f3,1}^1, \Delta t_{f3,1}^1 = T_1 + T_2 + T_3, t_{f3}^1 = t_1^1 + (T_1 + T_2 + T_3). \\
 t_{f4}^1 &= t_1^1 + \Delta t_{f4,1}^1, \Delta t_{f4,1}^1 = 2(T_1 + T_2 + T_3), t_{f4}^1 = t_1^1 + 2(T_1 + T_2 + T_3).
 \end{aligned}$$

$\Delta t_{f2,1}^1$, $\Delta t_{f3,1}^1$, and $\Delta t_{f4,1}^1$ are the time required for the fault signal to propagate to the corresponding observation point after the occurrence of the fault, and $\Delta t_{f4,1}^1 = 2 * \Delta t_{f2,1}^1 = 2 * \Delta t_{f3,1}^1$, which reflects the temporal characteristics of the fault propagation.

According to the fault classification of the traction drive control system of CRH2 EMU, the observation point settings, and the composition of the execution time of the system on the signal, the time required for the propagation of the fault characteristics to different observation points when different faults of the traction drive control system containing traction motor faults occur can be obtained, as shown in Table 2.

Experiment results and analysis

Experimental platform

Experimental studies are conducted on the semi-physical platform of the CRH2 traction drive control system shown in Fig. 3 [23, 24]. The fault injection simulation platform can be downloaded on the website <http://gfist.csu.edu.cn/indexE.html>; it includes a real-time simulator, a fault-injection unit (FIU), a physical traction drive control unit (TCU),

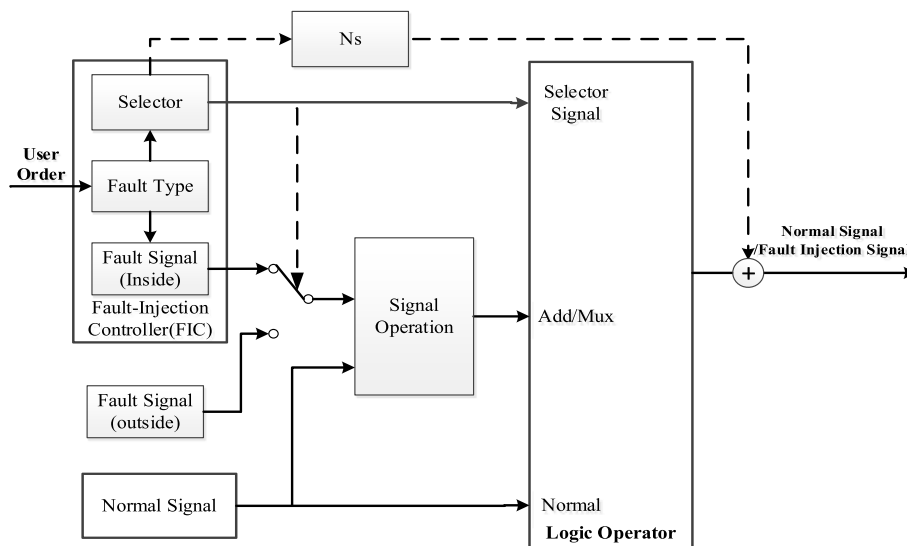


Fig. 4 Schematic diagram of the internal structure of the FIU

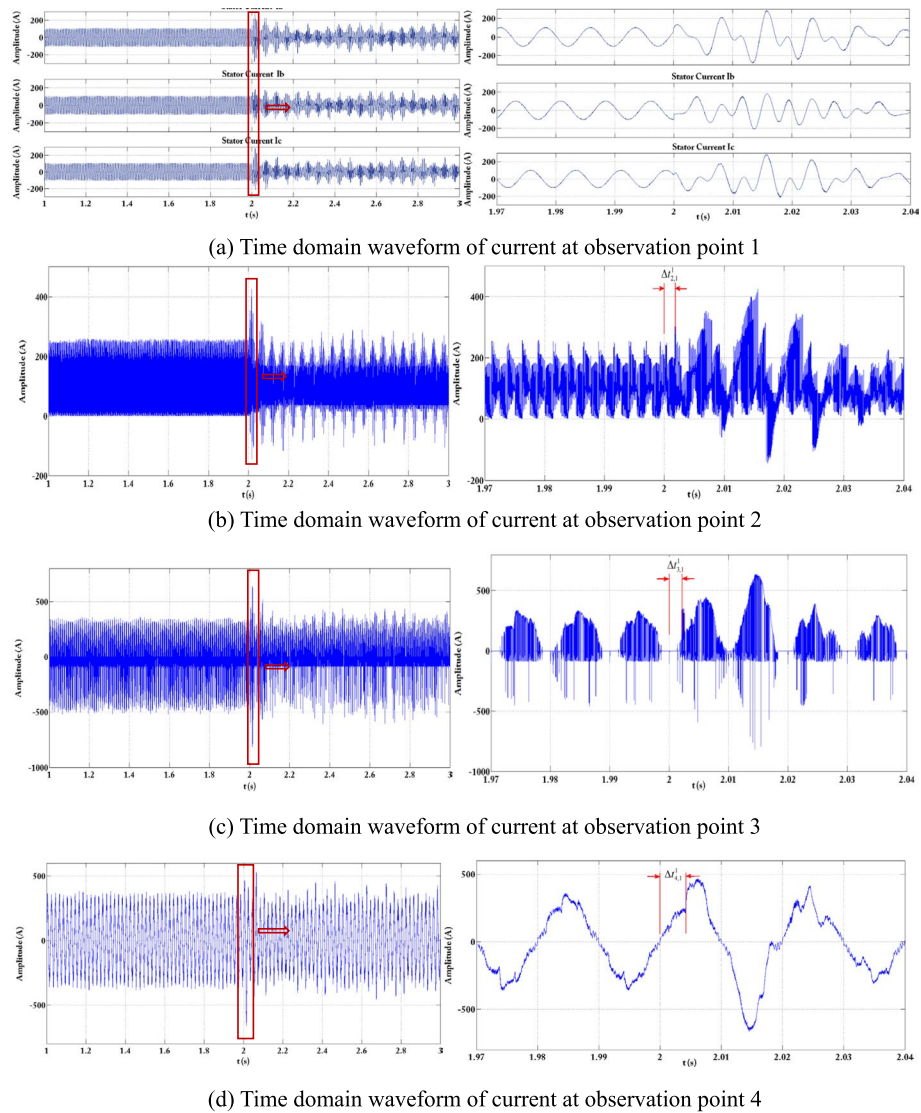


Fig. 5 Time domain waveforms of current at different observation points. **a** Time domain waveform of current at observation point 1. **b** Time domain waveform of current at observation point 2. **c** Time domain waveform of current at observation point 3. **d** Time domain waveform of current at observation point 4

and a real-time data acquisition and monitoring unit. The controller is a physical object. The dSPACE hardware includes a DS1007 CPU board, a DS5203 field-programmable gate array (FPGA) board, a DS4004 digital I/O board, and a DS2103 multichannel high-precision D/A board. Platform normal operation to 2 s was injected with different failure levels of traction motor rotor broken bar early weak faults.

The FIU consists of a fault injection controller (FIC), a signal processing unit, a logic solver, and a noise signal generator. The internal structure of the FIU is shown in Fig. 3. The FIC includes a selection signal module, a fault mode module, a fault signal module (internal), and a fault signal module (external), the signal operation process includes signal superposition and signal conditioning, the logic solver includes a logic operation

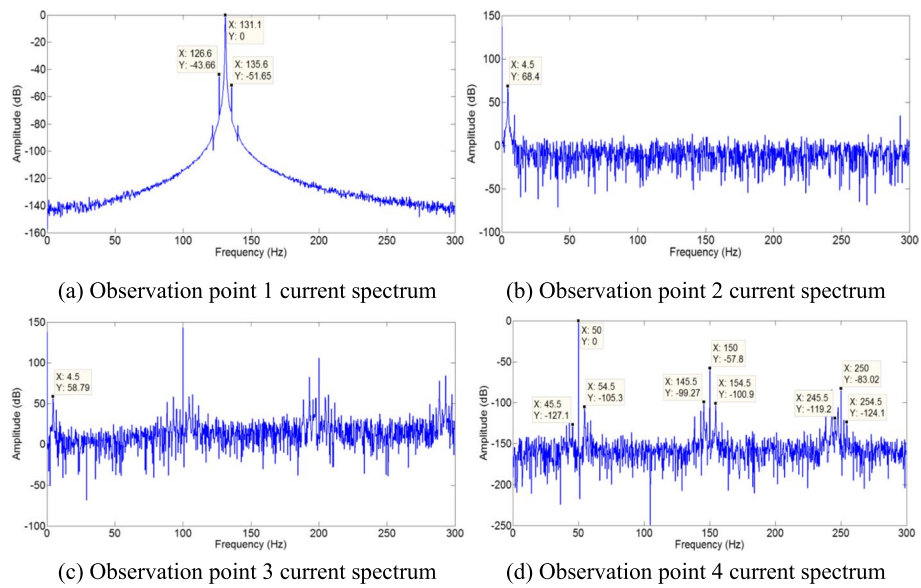


Fig. 6 Current spectrum of different observation points. **a** Observation point 1 current spectrum. **b** Observation point 2 current spectrum. **c** Observation point 3 current spectrum. **d** Observation point 4 current spectrum

section and a fault injection signal selection section, and the noise signal generator includes a noise signal generation module and a noise signal selection module.

Considering that the fault of the traction motor is destructive, its occurrence is random and influenced by many uncontrollable factors. Furthermore, the fault is an irreversible process, and the cost of man-made destruction of the motor is high. Currently, the simulation of traction motors for high-speed trains mainly focuses on normal operation, with a lack of in-depth research and simulation of faults. The fault injection method, however, can be employed to examine the faults of traction motors, enabling a more adaptable and cost-effective study.

Results and discussion

Figure 4 shows the current time domain waveforms of four different observation points of the traction drive control system. Each observation point contains two waveforms at the top and bottom, where the top graph shows the overall time domain graph of $1\text{ s} - 3\text{ s}$, and the bottom graph shows the local magnification of the area $1.97\text{ s} - 2.04\text{ s}$ in the top graph. The local detail graphs show that after a small defect in the previously weakened rotor bar, the defect features spread to different observation points of the system after a certain period of time.

The normalized spectrum analysis of the current signals of observation point 1, observation point 2, observation point 3, and observation point 4 under the fault condition is shown in Fig. 6.

Figure 5 displays the time domain current waveform at different observation points in the traction drive control system; during a weak, fault occurs in the pre-broken rotor of the traction motor. The partial magnification illustrates that fault characteristics propagate to different observation points of the system; after a certain time, the weak fault

occurs at the second s , observation point 1 finds the abnormality at the second s , observation point 2 finds the abnormality after time $\Delta t_{f2,1}^1$, observation point 3 finds the abnormality after time $\Delta t_{f3,1}^1$ found anomaly, and observation point 4 after time $\Delta t_{f4,1}^1$ found anomaly, and $\Delta t_{f2,1}^1 = \Delta t_{f3,1}^1 = 0.002s$ and $\Delta t_{f4,1}^1 = 0.004s$, satisfying $\Delta t_{f4,1}^1 = 2 * \Delta t_{f2,1}^1 = 2 * \Delta t_{f3,1}^1$, in accordance with the description of the time required for the propagation of different faults of the traction drive control system to different observation points in Table 2.

Figure 6 shows the current spectrum of observation point 1 to observation point 4 when the rotor of the traction motor is broken; it can be seen that there are obvious characteristic frequencies 126.6 Hz and 135.6 Hz on both sides of the stator current fundamental frequency 131.1 Hz of observation point 1, which is the characteristic frequency of the fault $(1 \pm 2s)f_1$; there are obvious characteristic frequencies 4.5 Hz of observation point 2 and observation point 3, which is the characteristic frequency of the fault $2sf_1$; and observation point 4 has obvious characteristic frequencies 45.5 and 54.5 on both sides of the rectifier input current fundamental frequency 50 Hz and 3 times the fundamental frequency 150 of the rectifier input current respectively. There are distinctive eigenfrequencies 45.5 Hz and 54.5 Hz on both sides of rectifier input current 50, 145.5 Hz and 154.5 Hz on both sides of rectifier input current 3 times the fundamental frequency 150 Hz, and 245.5 Hz and 254.5 Hz on both sides of rectifier input current 5 times the fundamental frequency 150 Hz, which are the fault eigenfrequencies $(4n \pm 1)f \pm 2sf_1$. The results of the spectral analysis of the current signals at different observation points are consistent with the theoretical calculation of the fault characteristic frequency values at different observation points in Table 1.

The fault propagation time and space characteristics are verified in Figs. 5 and 6, respectively. The fault occurrence frequency observed at the fault characteristic point suggests that the problem with the traction drive control system is a weak fault caused by a broken rotor bar in the pre-traction motor. Consequently, the location of the fault occurrence can be traced back to the traction motor, and the fault occurrence element is identified as the traction motor rotor guide bar, resulting in successful fault traceability.

Conclusions

To address deficiencies within the traction drive control system, we have implemented observation points and formulated a model with spatiotemporal characteristics via mechanism analysis. Furthermore, fault characteristics and propagation time were analyzed at different observation points for various types of faults. The fault characteristics and propagation time of the observation points are extracted and compared to the spatiotemporal characteristics of the corresponding observation points in the fault propagation model. This process enables the precise identification of the fault type and location, facilitating fault traceability. The experiment confirms that the technique presented in this paper is suitable for the control of traction transmission systems. It can successfully detect minor faults during system operation and furnish the operator with a dependable reference point for swiftly identifying the fault source and extent.

Acknowledgements

Not applicable.

Authors' contributions

All authors edited the manuscript and provided some references. All authors reviewed the results and approved the final version of the manuscript.

Funding

The research is supported by the following: Hunan Provincial Natural Science Foundation of China Project (2023JJ50270, 2023JJ50267, 2023JJ50263), Hunan Provincial Education Department Youth Project (21B0690), Hunan Provincial Science and Technology Department Science and Technology Project (2016TP1023), and Shaoyang Science and Technology Plan Project (2022GZ3034).

Hunan Provincial Natural Science Foundation of China Project, 2023JJ50270, Jintian Yin, 2023JJ50267, Li Liu, 2023JJ50263, Wu Shao, Hunan Provincial Education Department Youth Project, 21B0690, Jintian Yin, Hunan Provincial Science and Technology Department Science and Technology Project, 2016TP1023, Shaoyang Science and Technology Plan Project, 2022GZ3034, Li Liu

Availability of data and materials

All presented data are available under any request.

Declarations

Competing interests

The authors declare that they have no competing interests.

Received: 15 July 2023 Accepted: 3 November 2023

Published online: 23 November 2023

References

1. Chen HT, Jiang B, Steven XD et al (2022) Data-driven fault diagnosis for traction systems in high-speed trains: a survey, challenges, and perspectives. *IEEE T Intell Transp* 23(3):1700–1716. <https://doi.org/10.1109/TITS.2020.3029946>
2. Li QK, Ma X, Cui ML et al (2023) Fault diagnosis of bearings and gears based on LiteNet with feature aggregation. *IEEE T Instrum Meas* 72:1–9. <https://doi.org/10.1109/TIM.2023.3259032>
3. Sun YK, Cao Y, Li P (2022) Fault diagnosis for train plug door using weighted fractional wavelet packet decomposition energy entropy. *Accident Anal Prev* 166:106549. <https://doi.org/10.1016/j.aap.2021.106549>
4. Sun YK, Cao Y, Li P (2022) Contactless fault diagnosis for railway point machines based on multi-scale fractional wavelet packet energy entropy and synchronous optimization strategy. *IEEE T Veh Technol* 71(6):5906–5914. <https://doi.org/10.1109/TVT.2022.3158436>
5. Chen HT, Jiang B (2020) A review of fault detection and diagnosis for the traction system in high-speed trains. *IEEE T Intell Transp* 21(2):450–465. <https://doi.org/10.1109/TITS.2019.2897583>
6. Zhou CJ, Huang XF, Xiong NX (2015) A class of general transient faults propagation analysis for networked control systems. *IEEE T Syst Man Cy-S* 45(4):647–661. <https://doi.org/10.1109/TSMC.2014.2384480>
7. Ying Y, Peter BL, Krishna RP (2017) Fault diagnosis of HVAC air-handling systems considering fault propagation impacts among components. *IEEE T Autom Sci Eng* 14(2):705–717. <https://doi.org/10.1109/TASE.2017.2669892>
8. Chao MA, Kulkarni C, Goebel K et al (2021) Aircraft engine run-to-failure dataset under real flight conditions for prognostics and diagnostics. *Data* 6(1):5. <https://doi.org/10.3390/data6010005>
9. Wang RX, Gao X, Gao JM (2018) An information transfer based novel framework for fault root cause tracing of complex electromechanical systems in the processing industry. *Mech Syst Signal Pr* 101:121–139. <https://doi.org/10.1016/j.ymsp.2017.08.030>
10. Wang PK, Conrad JM, Amir MG (2018) An ATPG method for double stuck-at faults by analyzing propagation paths of single faults. *IEEE T Circuits-I* 65(3):1063–1074. <https://doi.org/10.1109/TCSI.2017.2765721>
11. Li J, Mark S, Jesus AP (2017) Fault signal propagation through the PMSM motor drive systems. *IEEE T Ind Appl* 53(3):2915–2924. <https://doi.org/10.1109/TIA.2017.2677881>
12. Wang T, Wei XG, Huang T (2019) Modeling fault propagation paths in power systems: a new framework based on event SNP systems with neurotransmitter concentration. *IEEE Access* 7:12798–12808. <https://doi.org/10.1109/ACCESS.2019.2892797>
13. Wang F, Xu TH, Tang T (2017) Bilevel feature extraction-based text mining for fault diagnosis of railway systems. *IEEE T Intell Transp* 18(1):49–58. <https://doi.org/10.1109/TITS.2016.2521866>
14. Gregory L, Xing LD, Hanoch BH (2013) Reliability of series-parallel systems with random failure propagation time. *IEEE T Reliab* 62(3):637–647. <https://doi.org/10.1109/TR.2013.2270415>
15. Bhusan M, Rengaswamy R (2002) Comprehensive design of a sensor network for chemical plants based on various diagnosability and reliability criteria, part 1: framework. *Ind Eng Chem Res* 41(7):1826–1839. <https://doi.org/10.1021/ie0104363>
16. Bhusan M, Rengaswamy R (2000) Design of sensor location based on various fault diagnostic observability and reliability criteria. *Comput Chem Eng* 24(2–7):735–741. [https://doi.org/10.1016/S0098-1354\(00\)00331-8](https://doi.org/10.1016/S0098-1354(00)00331-8)
17. Yang CH, Yang C, Peng T et al (2017) A fault-injection strategy for traction drive control systems. *IEEE T Ind Electron* 64(7):5719–5727. <https://doi.org/10.1109/TIE.2017.2674610>
18. Dou ZF, Wang N, Chen ZN et al (2023) An optimized MPC method for restraining the midpoint voltage fluctuation of 3-level T-type grid-connected inverter. *J Electr Eng Technol* 18(2):1111–1122. <https://doi.org/10.1007/s42835-022-01180-6>

19. Jose DV, Oscar C, Jaime JR et al (2018) Analysis of the response of L and LCL filters in controlled rectifiers used in wind generator systems with permanent magnet synchronous generators. *IEEE Lat Am T* 16(8):2145–2152. <https://doi.org/10.1109/TLA.2018.8528228>
20. Li Z, Feng GD, Lai CY et al (2021) Current injection-based simultaneous stator winding and PM temperature estimation for dual three-phase PMSMs. *IEEE T Ind Appl* 57(5):4933–4945. <https://doi.org/10.1109/TIA.2021.3091664>
21. Yin JT, Xie YF, Chen ZW et al (2019) Weak-fault diagnosis using state-transition-algorithm-based adaptive stochastic-resonance method. *J Cent South Univ* 26(7):1910–1920. <https://doi.org/10.1007/s11771-019-4123-6>
22. George G, Aicente VC, Jose AD et al (2017) The use of a multilabel classification framework for the detection of broken bars and mixed eccentricity faults based on the start-up transient. *IEEE T Ind Inform* 13(2):625–634. <https://doi.org/10.1109/TII.2016.2637169>
23. Yin JT, Xie YF, Peng T (2018) Current characteristics analysis and fault injection of an early weak fault in broken rotor bar of traction motor. *Math Probl Eng* 2018:1–8. <https://doi.org/10.1155/2018/4934720>
24. Peng T, Tao HW, Yang C et al (2019) A uniform modeling method based on open-circuit faults analysis for NPC-three-level converter. *IEEE T Circuits-II* 66(3):457–461. <https://doi.org/10.1109/TCSII.2018.2856862>

Submit your manuscript to a SpringerOpen[®] journal and benefit from:

- ▶ Convenient online submission
- ▶ Rigorous peer review
- ▶ Open access: articles freely available online
- ▶ High visibility within the field
- ▶ Retaining the copyright to your article

Submit your next manuscript at ▶ [springeropen.com](https://www.springeropen.com)
